

Midgut epithelium in molting silkworm: A fine balance among cell growth, differentiation, and survival



Eleonora Franzetti^a, Morena Casartelli^b, Paola D'Antona^a, Aurora Montali^a, Davide Romanelli^a, Silvia Cappellozza^c, Silvia Caccia^{b,d}, Annalisa Grimaldi^a, Magda de Eguileor^a, Gianluca Tettamanti^{a,*}

^a Department of Biotechnology and Life Sciences, University of Insubria, 21100 Varese, Italy

^b Department of Biosciences, University of Milano, 20133 Milano, Italy

^c CREA – Honey Bee and Silkworm Research Unit, Padua Seat, 35143 Padova, Italy

^d Department of Agricultural Sciences, University of Napoli Federico II, 80055 Portici, Italy

ARTICLE INFO

Article history:

Received 27 February 2016

Accepted 22 June 2016

Available online 8 July 2016

Keywords:

Autophagy

Insect midgut

Lepidoptera

Molt

Intestinal stem cells (ISCs)

ABSTRACT

The midgut of insects has attracted great attention as a system for studying intestinal stem cells (ISCs) as well as cell death-related processes, such as apoptosis and autophagy. Among insects, Lepidoptera represent a good model to analyze these cells and processes. In particular, larva–larva molting is an interesting developmental phase since the larva must deal with nutrient starvation and its organs are subjected to rearrangements due to proliferation and differentiation events. Several studies have analyzed ISCs *in vitro* and characterized key factors involved in their division and differentiation during molt. However, *in vivo* studies performed during larva–larva transition on these cells, and on the whole midgut epithelium, are fragmentary.

In the present study, we analyzed the larval midgut epithelium of the silkworm, *Bombyx mori*, during larva–larva molting, focusing our attention on ISCs. Moreover, we investigated the metabolic changes that occur in the epithelium and evaluated the intervention of autophagy.

Our data on ISCs proliferation and differentiation, autophagy activation, and metabolic and functional activities of the midgut cells shed light on the complexity of this organ during the molting phase.

© 2016 Elsevier Ltd. All rights reserved.

1. Introduction

In insects, postembryonic development is characterized by alternating between feeding and molting stages, the latter culminating in ecdysis. During this process, the insect loosens the connections between its living tissues and the extracellular cuticle, escapes from it, takes up water or air to expand the new, flexible exoskeleton, and then quickly hardens it for purposes of defense and locomotion (Wigglesworth, 1972). This is a life-threatening process since a failure in the sequence of events, which are triggered by hormones and involve the coordinated expression of a

wide array of genes, can result in the insect's death (Riddiford et al., 2003; Zhao et al., 2006). Together with the growth that occurs during the intermolt period, the gain in size during the intramolt phase (molt increment) also contributes to the growth of the insect body (Gullan and Cranston, 2014). In insects, different types of stem cells are recruited during molting to promote the growth and remodeling of the larval organs (Corley and Lavine, 2006). In this context, the larval midgut of holometabolous insects is no exception.

The alimentary canal of the larva is subdivided into three major regions, namely, the foregut, the midgut, and the hindgut, which have different functional roles in feeding and digestion. The foregut is primarily responsible for food ingestion and storage, the hindgut is implicated in the osmotic regulation of internal fluids, while the midgut is involved in nutrient digestion and absorption (Dow, 1986). In lepidopteran larvae, the midgut consists of a

* Corresponding author. Department of Biotechnology and Life Sciences, University of Insubria, Via J. H. Dunant, 3, 21100 Varese, Italy. Tel.: +39 0332 421312; fax: +39 0332 431300.

E-mail address: gianluca.tettamanti@uninsubria.it (G. Tettamanti).

monolayered epithelium essentially formed by columnar cells, which produce digestive enzymes and absorb nutrients, and goblet cells, which are involved in ion transport (Terra and Ferreira, 2005). Two other cell types are found in the midgut, namely, endocrine and intestinal stem cells (ISCs). Endocrine cells are sparse in the epithelium and produce the gastrointestinal hormones needed to control the production and secretion of digestive enzymes and for proliferation and differentiation of ISCs (Sehnal and Zitnan, 1996; Rost-Roszkowska et al., 2008). ISCs reside on the basal lamina that supports the epithelium, among columnar and goblet cells. ISCs repair the damaged midgut by replacement in order to maintain the functional integrity of the tissue (Smagghe et al., 2005; Hakim et al., 2010). In addition to the repair function, ISCs proliferate extensively at each larva–larva molt and then intercalate between the mature cells, differentiating into columnar and goblet cells (Baldwin and Hakim, 1991b; Baldwin et al., 1996). A third role of ISCs is to generate a new functional midgut at larva–pupa molting, which is maintained up to the adult stage (Tettamanti et al., 2007a; Franzetti et al., 2015). In the last few decades, studies on cultured stem cells derived from the midgut of different lepidopteran species have provided insights into the factors that control proliferation and differentiation of these cells (Smagghe et al., 2003; Blackburn et al., 2004; Loeb et al., 2004; Smagghe et al., 2005). This work yielded important information about the setup of midgut primary cultures (Casartelli et al., 2007; Hakim et al., 2009) and their use as a tool to study the physiological properties of midgut cells *in vitro* (Casartelli et al., 2008).

While the *in vitro* investigation reported above has helped us to better understand some of the regulatory mechanisms involved in the proliferation and differentiation of ISCs, *in vivo* studies are scarce. In particular, although the behavior of these stem cells during the larva–pupa transition has been characterized in detail (Uwo et al., 2002; Tettamanti et al., 2007a, 2008; Franzetti et al., 2012; Franzetti et al., 2015), only little information is available on ISCs during the larva–larva molting phase and, more in general, on the events occurring in the larval midgut epithelium during this larval developmental process (Baldwin and Hakim, 1991a, 1991b; Baldwin et al., 1993). Moreover, it is worthy of note that a proteomic study performed in *Helicoverpa armigera* molting larvae did not identify any obvious, differentially expressed protein spots in the midgut, thus suggesting that minor metabolic changes occur in this organ during larva–larva molt (Zhao et al., 2006). This evidence undoubtedly adds further complexity to the analysis of the whole organ. This lack of, or only fragmentary knowledge could hinder the full exploitation of lepidopteran midgut as a model system to study stem cell biology. Furthermore, full characterization of the events that occur in the midgut during larval–larval molting would provide additional advantages. In particular, during this developmental phase, the insect stops feeding, thus offering an opportunity to study the metabolic processes that are set in motion in this organ by physiological starvation.

In the present work (i) we studied the morphology and functional activity of the midgut epithelium of the silkworm, *Bombyx mori*, during larva–larva molting (IV to V larval instar), focusing our attention on ISCs; (ii) we analyzed the metabolic changes that occur in this organ; and (iii) we evaluated the activation of autophagy, a self-eating process that can be used by eukaryotic cells to cope with nutrient deprivation (He and Klionsky, 2009).

To our knowledge, this study represents the first morphological and functional characterization of the changes that occur in the midgut of a lepidopteran during larva–larva molt. Our results not only provide important insights into the field of stem cell biology, but also represent a useful reference for further studies on molt processes.

2. Materials and methods

2.1. Experimental animals

B. mori (polyhybrid strain (126 × 57) (70 × 90)) larvae were provided by CREA – Honey Bee and Silkworm Research Unit (Padova, Italy). The larvae were fed on artificial diet (Cappelozza et al., 2005) and reared at 25 ± 0.5 °C under a 12:12 h light:dark period and 70% relative humidity. The silkworm life cycle includes five larval instars separated by molts. At the end of the larval period, the animal undergoes a larval–pupal molt and initiates metamorphosis. Each larval stage lasts about four days, each larva–larva molting approximately 24 h. Since the processes that regulate the growth of organs at each larva–larva molting are conserved (Baldwin et al., 1996), we examined larva–larva molting from fourth to fifth instar in the present study. Here, owing to the considerable dimensions of the larvae, the midgut could be appropriately manipulated.

Larvae at the following stages were selected and used for the analyses:

- L4D3 and L4D4: third and fourth day of the fourth larval instar;
- Stage I: early molting larvae (0–12 h). Initiation of molting phase was determined by assessing the presence of visible signs of molting (initial detachment of the head capsule from the body cuticle);
- Stage II: late molting larvae (12–24 h). End of molting was assessed by the complete loss of the exuvia;
- L5D1: first day of the fifth larval instar.

2.2. Light microscopy and transmission electron microscopy (TEM)

The midgut was isolated from larvae anesthetized with CO₂ and immediately fixed in 4% glutaraldehyde (in 0.1 M Na-cacodylate buffer, pH 7.4) overnight at 4 °C. After postfixation in 1% osmium tetroxide for 1 h, samples were dehydrated in an ethanol series and embedded in resin (Epon/Araldite 812 mixture). Semithin sections were stained with crystal violet and basic fuchsin and observed by using a Nikon Eclipse Ni-U microscope equipped with a DS-5M-L1 digital camera system (Nikon, Tokyo, Japan). Ultrathin sections were stained with uranyl acetate and lead citrate and examined by using a Jeol JEM-1010 electron microscope (Jeol, Tokyo, Japan) equipped with an Olympus Morada digital camera (Olympus, Münster, Germany).

2.3. Morphometric analysis

In order to count the number of ISCs in the midgut epithelium, images of midgut samples from larvae at the end of fourth instar (L4D4) and Stage I, randomly taken at optical microscope (50 × magnification), were morphometrically analyzed. Two hundred images in total (five larvae; ten sections per larva; four images per section) were evaluated for each developmental stage. These sections were at a minimum distance of 50 μm from each other, to avoid counting the same cells twice. For each image, a 100-μm line segment was selected on the basal lamina of the midgut and the number of ISCs localized on this portion of the epithelial layer was counted by using ImageJ software (NIH, Bethesda, USA). Data were analyzed using the Student's *t* test. Results are expressed as the number of ISCs per 100 μm epithelium.

2.4. Histochemistry

2.4.1. NADH-dehydrogenase and oil red O

Midgut samples were embedded in polyfreeze cryostat embedding medium after dissection and stored in liquid nitrogen until use. Then, 8- to 10- μ m-thick cryosections were obtained with a Leica CM 1850 cryostat and slides were used immediately or stored at -20°C . Sections were processed with Bio-Optica Histopathological kit (Bio-Optica, Milano, Italy) to detect NADH-dehydrogenase (NADH-TR) (EC 1.6.99.3) activity and to demonstrate lipid droplets (Oil red O staining, O.R.O.) in the midgut tissue. Stainings were performed according to the manufacturer's instructions.

2.4.2. Periodic acid-Schiff and alkaline phosphatase

Samples of midgut were fixed in paraformaldehyde (4% in phosphate-buffered saline (PBS)) (137 mM NaCl, 2.7 mM KCl, 10 mM Na_2HPO_4 , 2 mM KH_2PO_4 , pH 7.4) for 3 h at room temperature. Specimens were dehydrated in an ethanol series and embedded in paraffin (Franzetti et al., 2015). To detect glycogen in the midgut tissue, 8- μ m-thick sections were deparaffinized by treatment with Bioclear (Bio-Optica) and rehydrated in an ethanol series. They were then processed for Periodic acid-Schiff (PAS) staining in combination with diastase (PAS-D), which breaks down glycogen, according to the manufacturer's instructions (Bio-Optica Histopathological kit). To detect alkaline phosphatase (EC 3.1.3.1) activity in the midgut epithelium, deparaffinized sections were incubated with BCIP/NBT substrate (Sigma–Aldrich, St. Louis, MO, USA) (Miao and Scutt, 2002).

2.5. Analysis of mitotic cells

An anti-H3P antibody was used to analyze the cell division process that takes place in the midgut epithelium. Unlike cell proliferation assays (i.e., incorporation of BrdU or 3H-thymidine, or detection of PCNA), this marker recognizes mitotic cells and is thus more suitable to demonstrate the presence of dividing cells (Franzetti et al., 2015).

2.5.1. Immunohistochemistry

Cryosections (see paragraph 2.4.1) were washed in PBS for 5 min to remove polyfreeze cryostat embedding medium. After a 30-min incubation with a blocking solution (2% bovine serum albumin, 0.01% Tween 20 in PBS), they were incubated with an anti-phospho-histone H3 (H3P) antibody (dilution 1:100; Merck-Millipore, Billerica, MA, USA) for 2 h at room temperature. After extensive washes, specimens were incubated with an anti-rabbit Cy5-conjugated secondary antibody (dilution 1:50; Jackson Immuno Research Laboratories, West Grove, PA, USA) for 1 h at room temperature. Nuclei were revealed by DAPI staining (100 ng/ml). Primary antibody was omitted in control samples, and sections were treated with blocking solution. Coverslips were mounted with Citifluor (Citifluor, London, UK) and slides were examined with a Nikon Ni-U microscope.

2.5.2. Western blot analysis

Midguts were homogenized with a T10 basic ULTRA-TURRAX (IKA, Staufen, Germany) in 1 ml/0.1 g tissue of RIPA buffer (150 mM NaCl, 1% NP-40, 0.5% sodium deoxycholate, 0.1% SDS, 50 mM Tris, pH 8.0), to which 1 \times protease inhibitor cocktail (Sigma–Aldrich) was added. Particulate material was removed by centrifugation at 15,000 \times g for 15 min at 4 $^{\circ}\text{C}$. Supernatants were denatured by boiling the samples in 2 \times gel loading buffer for 5 min. SDS-PAGE was performed on a 12% acrylamide gel by loading 40 μ g protein per lane. After electrophoretic separation, proteins were

transferred onto PVDF membranes (Merck-Millipore). Membranes were saturated with a solution of 5% milk and 0.1% Tween 20 in Tris-buffered saline (TBS) (50 mM Tris–HCl, 150 mM NaCl, pH 7.5) overnight at 4 $^{\circ}\text{C}$ and subsequently incubated for 2 h at room temperature with the following antibodies: anti-H3P (dilution 1:500; Merck-Millipore), anti-ATG8 (dilution 1:500) (Franzetti et al., 2012), and anti-GAPDH (dilution 1:2500; Proteintech, Chicago, IL, USA) to ensure equal gel loading. Antigens were detected with an anti-rabbit HRP-conjugated secondary antibody (dilution 1:7500; Jackson Immuno Research Laboratories) and immunoreactivity with SuperSignal chemiluminescence substrates (Thermo Fisher Scientific).

2.6. Enzyme assays

To analyze the functional capabilities of the silkworm midgut epithelium during larva–larva molt, we evaluated the activity of alkaline phosphatase, a specific marker for the apical plasma membrane in absorptive epithelia (Terra and Ferreira, 2005). We also measured the activity of aminopeptidase N, a hydrolytic enzyme that is involved in the intermediate and final digestion of proteins and highly represented in apical membranes of absorbing epithelia (Terra and Ferreira, 1994).

Midguts were dissected on ice and, after a rinse in a Saline Solution for Lepidoptera (SSL) (210 mM Sucrose, 45 mM KCl, 10 mM Tris–HCl, pH 7.0), were stored in liquid nitrogen until use. After thawing, samples were homogenized (nine strokes at 2000 rpm in a glass-Teflon Potter homogenizer) in 1 ml/0.1 g tissue of the following homogenization buffer: 100 mM mannitol, 10 mM Hepes–Tris at pH 7.2. A protease inhibitor cocktail (Sigma–Aldrich) was added during the homogenization procedure. The protein concentration in the homogenates was determined by using Coomassie Brilliant Blue G-250 protein assay (Thermo Fisher Scientific), with BSA as standard.

Assays of the enzyme activities in the homogenates were performed (at least in quadruplicate) at 25 $^{\circ}\text{C}$ on a Pharmacia Biotech Ultrospec 3000 spectrophotometer with a thermostatic cuvette holder.

Alkaline phosphatase (EC 3.1.3.1) activity was determined by measuring the release of p-nitrophenol from p-nitrophenylphosphate (2 mM) in 1 M Tris–HCl, pH 8, at 400 nm. Aminopeptidase N (EC 3.4.11.2) activity was evaluated by measuring the release of p-nitroaniline from L-leucine-p-nitroanilide (4 mM) in 40 mM Tris–HCl, pH 7.5, at 410 nm.

2.7. Quantitative real-time PCR (qRT-PCR)

Larvae from the third day of the fourth larval instar up to L5D1 were used for qRT-PCR analysis. The midgut was dissected from the larvae, immediately frozen in liquid nitrogen, and stored at -80°C until use. Total RNA was extracted from 20 to 40 mg of tissue using

Table 1
Sequence of primers used in this study.

Gene name	Genbank number	Primer sequence
<i>BmATG1</i>	NM_001309546.1	F: CCCCGCTATGCTCTATGTTG R: ATCTGATGGGTGGGAGTACG
<i>BmATG5</i>	NM_001142487.1	F: TTGGACTTTAATGGGCAACC R: CATCTTGTGGGCAATGA
<i>BmATG6</i>	NM_001142490.1	F: TGCTCTCTCTCTCGTTAGCC R: AGCCCGTATTACCCATTCC
<i>BmATG8</i>	NM_001046779.1	F: CCAGATCGCGTCTCTGTAAT R: GAGACCCCATTTGTGCAGAT
<i>BmRP49</i>	NM_001098282.1	F: AGGCATCAATCGGATCGCTATG R: TTGTGAAGTACGACCTTACGGAATC

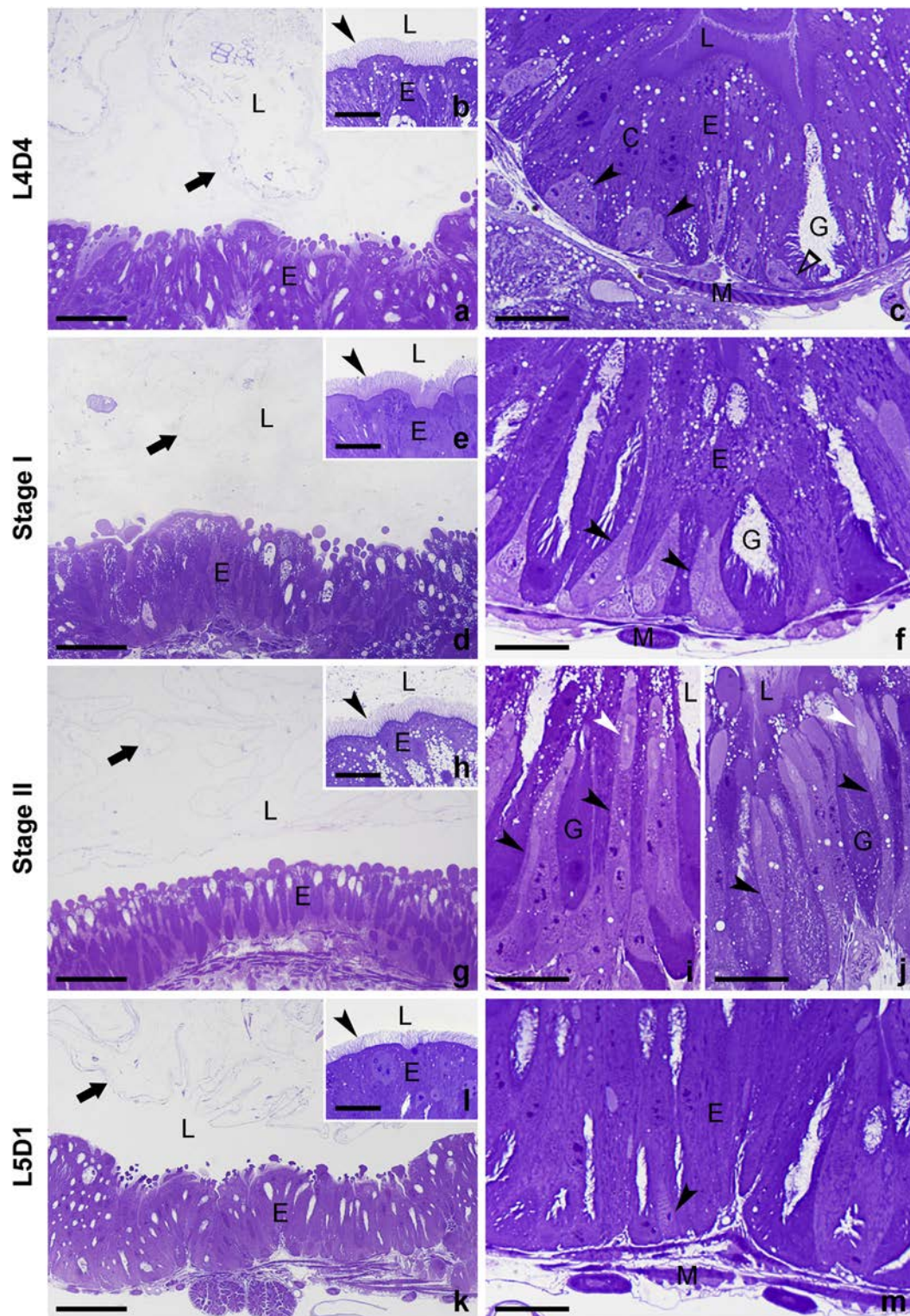
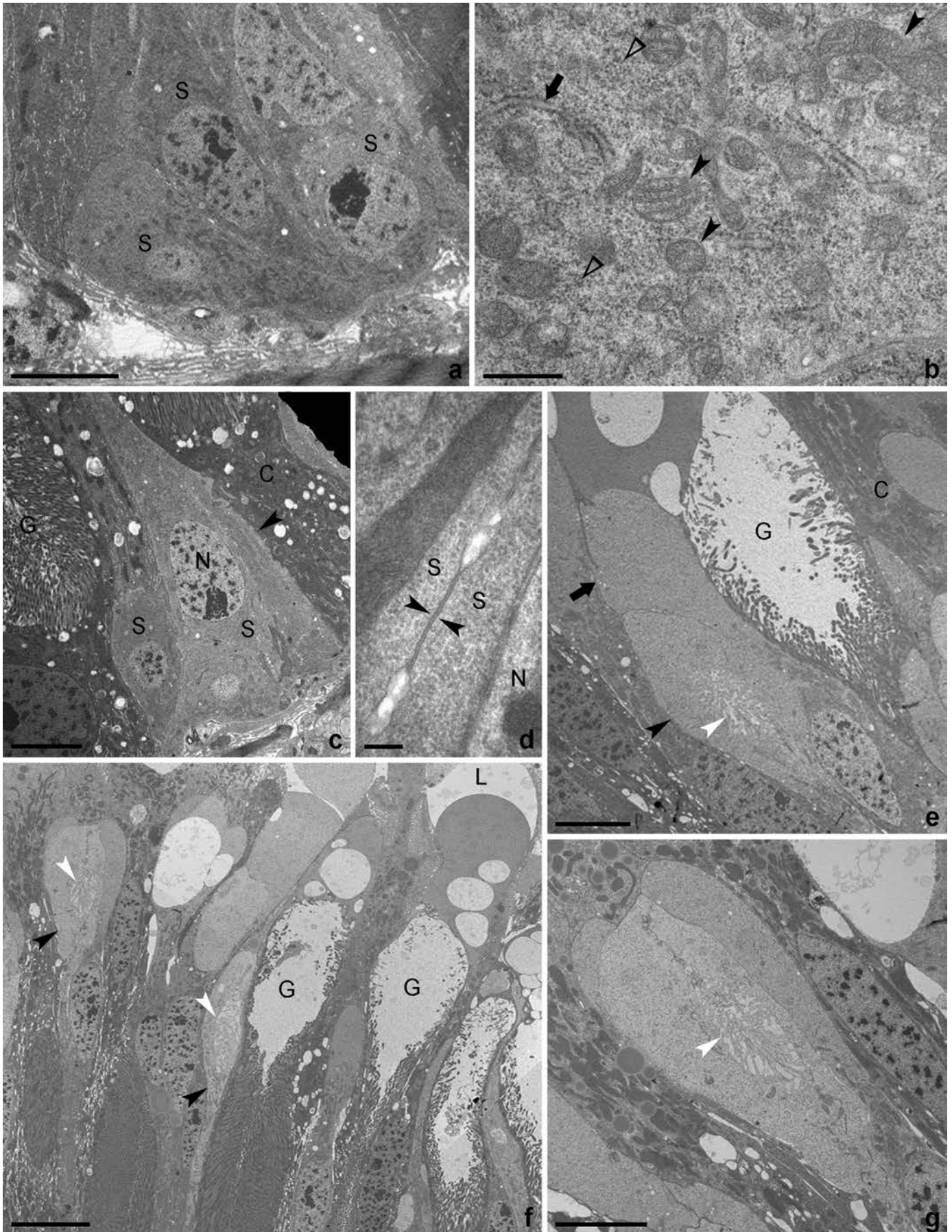


Fig. 1. Structure of the larval midgut epithelium during larva–larva molt. Semithin cross-sections. During fourth larval instar, the midgut consists of a monolayered epithelium (E), surrounded by muscle fibers (M), in which columnar (C) and goblet (G) cells can be observed (a, c). Sparse (open arrowhead) ISCs or ISCs organized in small nidi (arrowheads) are localized in the basal region of the epithelium (c). Although the general structure of the epithelium is maintained during molt (d, g), from stage I onwards stem cells proliferate and differentiate into new mature cells that intercalate among pre-existing columnar and goblet cells (f, i, j, arrowheads). Cells undergoing differentiation can be clearly distinguished from mature cells due to their light color (f, i, j, arrowheads). Those cells that will give rise to goblet cells show an apical intracellular cavity (i, j, white arrowheads). At the beginning of the fifth larval instar, only few isolated ISCs are visible in the basal region of the epithelium (m, arrowhead). Peritrophic matrix (a, d, g, k, arrow) and a well-developed brush border in the apical region of the epithelium (b, e, h, i, arrowhead) remain visible at all the stages analyzed. L: lumen. Bars 100 μm (a, d, g, k), 20 μm (b, c, e, f, h, i, j, l, m).



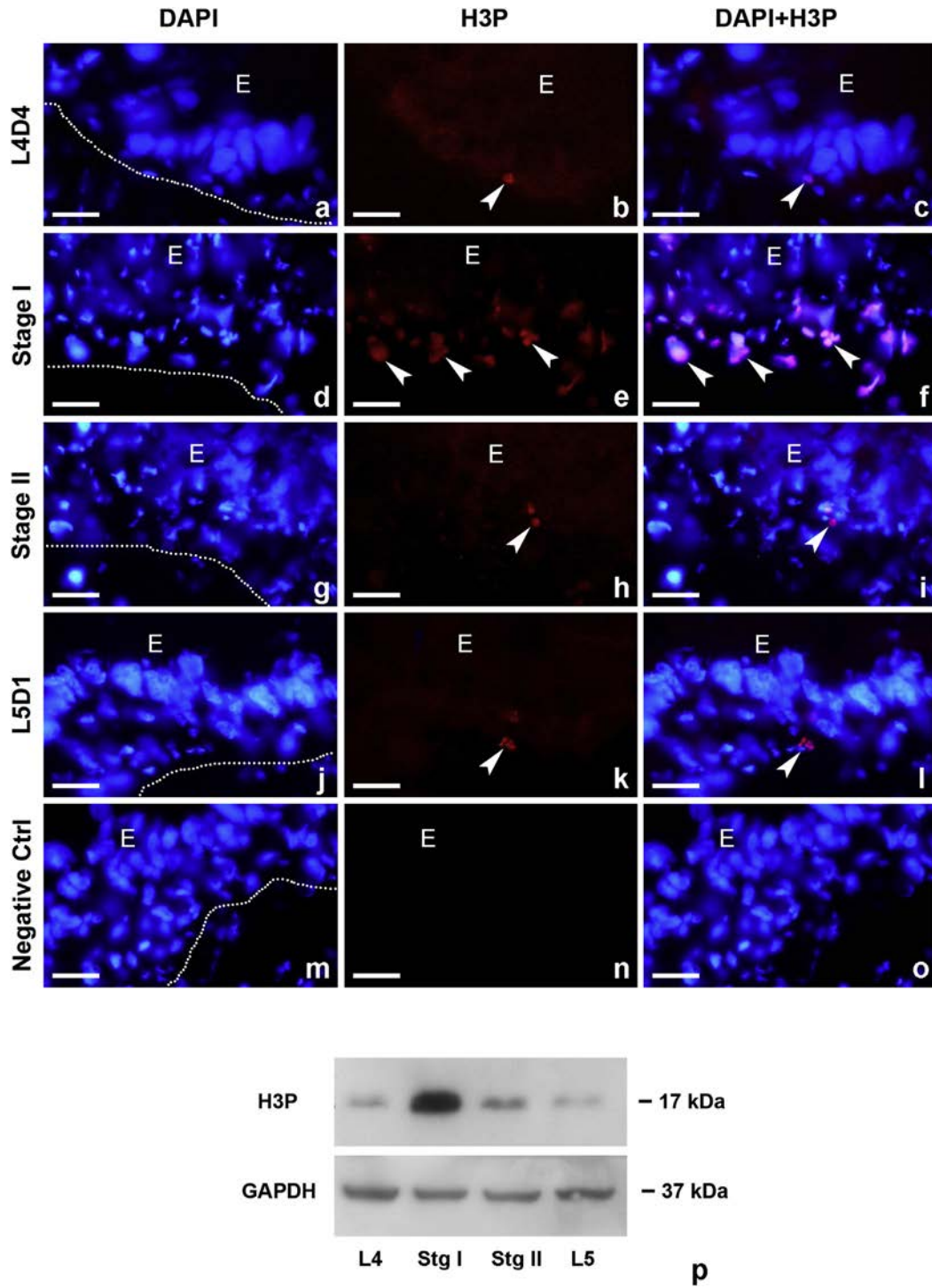


Fig. 3. Proliferation of ISCs during molt. (a–o) Immunolocalization of H3P antibody. At fourth larval instar, the antibody reveals a weak positivity (arrowheads) for H3P (a–c). During stage I, a strong signal is visible in cells localized in the basal region of the epithelium (d–f). At later stages, the number of positive cells is limited (g–l). No staining can be observed in negative controls (m–o). c, f, i, l, o have been obtained by overlapping the DAPI signal (a, d, g, j, m) onto H3P positivity (b, e, h, k, n). Dotted line indicates the basal end of the epithelium. DAPI-positive nuclei that are visible below the dotted line belong to muscle cells. (p) Western blot analysis of H3P. The antibody specific for H3P recognizes a 17-kDa band, whose intensity is very high at stage II. E: midgut epithelium. Bars 30 μm (a–o).

Fig. 2. Differentiation of ISCs during molt. TEM. At L4D4, ISCs (S) are organized in small groups (a). In their cytoplasm abundant mitochondria (arrowheads) and ribosomes (open arrowheads) are visible, while RER (arrow) is scarcely represented (b). From stage I, ISCs start to differentiate: they elongate (c, arrowhead), join each other by junctions (d, arrowheads), and intercalate among mature cells (e). Differentiating cells extend up to the midgut lumen (f, arrowheads). While ISCs that give rise to columnar cells maintain their elongated shape (e, arrow), ISCs that generate goblet cells (e, arrowhead) show an intracellular cavity that is lined by microvilli (e, g, white arrowhead). C: columnar cell; G: goblet cell; L: lumen; N: nucleus. Bars 5 μm (a, c, e, g), 500 nm (b), 200 nm (d), 10 μm (f).

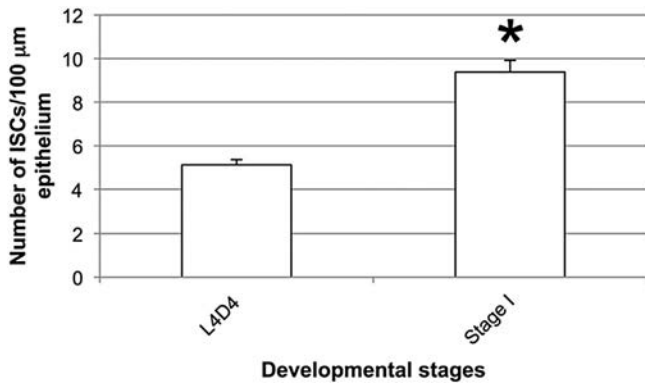


Fig. 4. Morphometric analysis showing the number of ISCs in the midgut epithelium of L4D4 and stage I larvae. During the transition from fourth larval instar to early molting phase, a significant increase in the number of stem cells is observed. Data are represented as mean \pm SE; * $p < 0.001$.

Trizol Reagent (Life Technologies, Carlsbad, USA) according to the manufacturer's instructions with slight modifications. RNA was treated with TURBO DNA-free Kit (Life Technologies) to remove any genomic DNA contamination and its integrity was assessed by electrophoresis. RNA was retrotranscribed using M-MLV reverse transcriptase (Life Technologies). qRT-PCR primers were designed for *BmATG1* (NM_001309546.1), *BmATG5* (NM_001142487.1), *BmATG6* (NM_001142490.1), *BmATG8* (NM_001046779.1), and *BmRP49* (NM_001098282.1). The primers used are indicated in Table 1. qRT-PCR was performed with iTaq Universal SYBR Green Supermix (Biorad, Hercules, CA, USA) using a 96-well CFX Connect Real-Time PCR Detection System (Biorad). The $2^{-\Delta\Delta C_t}$ method, with *BmRP49* as housekeeping gene, was used to calculate the relative expression of the four *ATG* genes during molt. Each value was the result of measurements performed on midguts from three series of animals. Relative expression was calculated and statistical analysis performed using Biorad CFX Manager Software (Biorad).

3. Results

3.1. Growth and modification of the midgut epithelium during molt

The general morphology of the midgut epithelium was maintained throughout the molting period (Fig. 1a, d, g and k). This tissue was layered by a peritrophic matrix that remained visible at all stages analyzed. The aspect of this acellular structure remained almost unchanged from L4D4 up to the beginning of the fifth larval instar (Fig. 1a, d, g and k).

By analyzing the midgut epithelium at higher magnification we could observe modifications of this tissue at the cellular level (Fig. 1b, c, e, f, h, i, j, l and m). At the end of fourth larval instar, the epithelium was formed by columnar and goblet cells. In the basal region of the epithelial monolayer, sparse ISCs or cells grouped in small nidi were visible (Fig. 1c). At TEM these cells appeared pear-shaped and were characterized by an undifferentiated morphology (Fig. 2a): their cytoplasm contained numerous ribosomes and mitochondria, while RER was poorly developed (Fig. 2b). Owing to all of these features, ISCs could be clearly distinguished from the remaining epithelial cells. During stage I, the number of ISCs increased (Figs. 1f and 4) and they became differentiated (Figs. 1f and 2c): ISCs grew towards the midgut lumen by intercalating among columnar and goblet cells (Figs. 1i, j and 2e, f), spanning the entire thickness of the epithelium (Figs. 1j and 2f). Cells undergoing differentiation could be easily recognized since they were light-

colored (light microscopy) (Fig. 1f, i and j) and electron-lucent (TEM) (Fig. 2c, e and f). From the early stage of differentiation, these cells appeared to be linked to each other by septate junctions (Fig. 2d). At later stages, in those ISCs that gave rise to goblet cells, it was possible to observe an intracellular cavity lined by microvilli: this, after a progressive expansion, transformed into the typical cavity visible in mature goblet cells (Fig. 2e–g). In contrast, ISCs that generated columnar cells maintained their elongated shape (Fig. 2e). At the beginning of fifth larval instar (L5D1), the newly differentiated cells were almost indistinguishable from the mature columnar and goblet cells that were already present in the epithelium at the beginning of the molt, while isolated ISCs were still visible in the basal region (Fig. 1m).

In order to characterize the cell division process that occurs in the midgut epithelium, we used an anti-H3P antibody. Immunostaining performed on midgut sections showed a different amount of H3P-positive cells in the epithelium along the molt. In particular, while numerous H3P-positive nuclei were visible at stage I, the staining was almost absent in all the remaining samples analyzed (Fig. 3a–o). It must be noted that the signal was localized in the basal region of the epithelium and could thus be ascribed to ISCs (Fig. 3b, c, e, f, h, i, k and l). To better evaluate the levels of this mitotic marker in the overall midgut epithelium, we performed western blot analysis. The antibody recognized a 17-kDa band and confirmed the pattern seen in immunostaining. In fact, although limited mitotic activity was visible from L4D4 onwards, an intense H3P signal was found only at stage I (Fig. 3p). The proliferation of ISCs at the beginning of the molt was confirmed by morphometric analysis: in fact, a significant increase in the number of these cells was observed during the transition from L4D4 to stage I (Fig. 4).

These data indicate that the maximum rate of stem cell mitosis occurs within 12 h after the molt begins and that, soon after, differentiating cells grow within the midgut cell layer to widen the epithelium.

3.2. Analysis of the functional activity of the midgut

Alkaline phosphatase and aminopeptidase N were used to investigate the functional capabilities of the midgut epithelium during molting. The histochemical assay for alkaline phosphatase revealed a signal in the apical region of the epithelium that showed a different intensity, depending on the stage analyzed. In particular, while the intensity of the staining at L4D4 and L5D1 was comparable, it decreased during molting (stage I and II) (Fig. 5a–d). The activity of this enzyme was quantified by using a spectrophotometric assay to confirm the histochemical evidence. As shown in Fig. 5e, the activity of this enzyme was detected from L4D4 to L5D1, although a significant decrease was recorded during the molt period. At the beginning of fifth larval instar, alkaline phosphatase activity was comparable to that observed in midgut samples isolated from fourth instar larvae (Fig. 5e). The pattern of aminopeptidase N activity was similar to that of alkaline phosphatase (Fig. 5f), confirming that, although at reduced levels, the functional activity of the epithelium was maintained during the molt period.

We also analyzed the structure of the apical brush border and monitored mitochondrial activity in midgut cells, two parameters that are directly related to the activity of the epithelium. Morphological analysis revealed the presence of a well-developed brush border in columnar cells along the molt period (Fig. 1b, e, h and l), and NADH-TR confirmed that the mitochondrial activity of midgut cells did not decrease for the entire duration of the molt (Fig. 5g–j).

All the collected data are consistent with an epithelium that can fulfill digestive and absorption functions also during molting, a 24-h period during which the larvae do not ingest food.

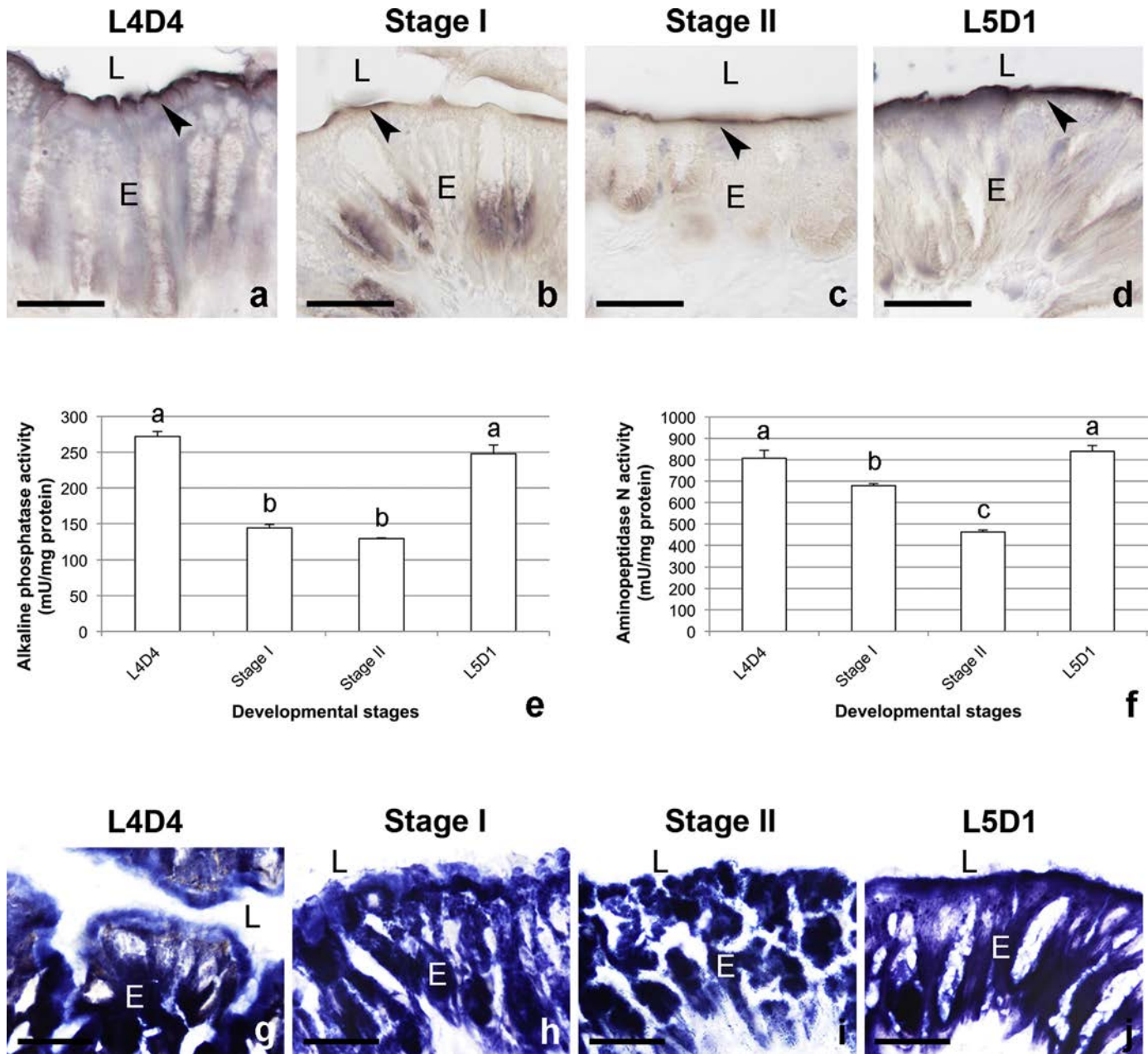
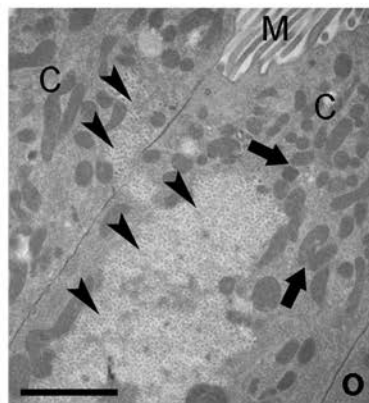
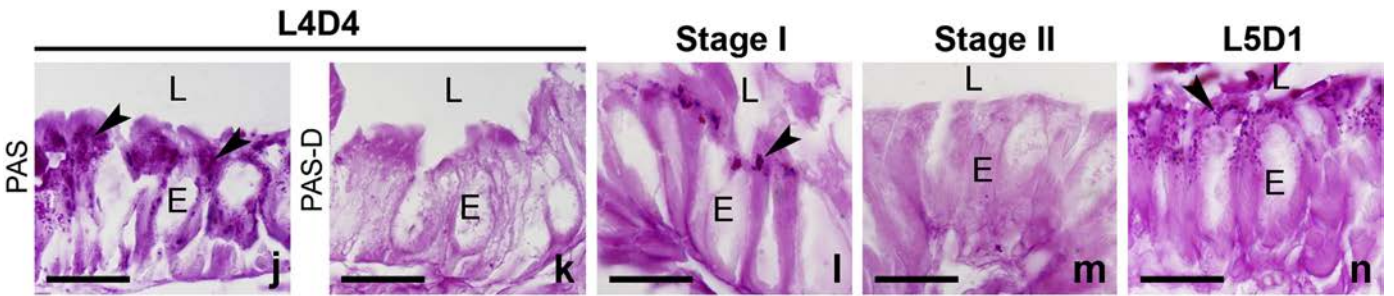
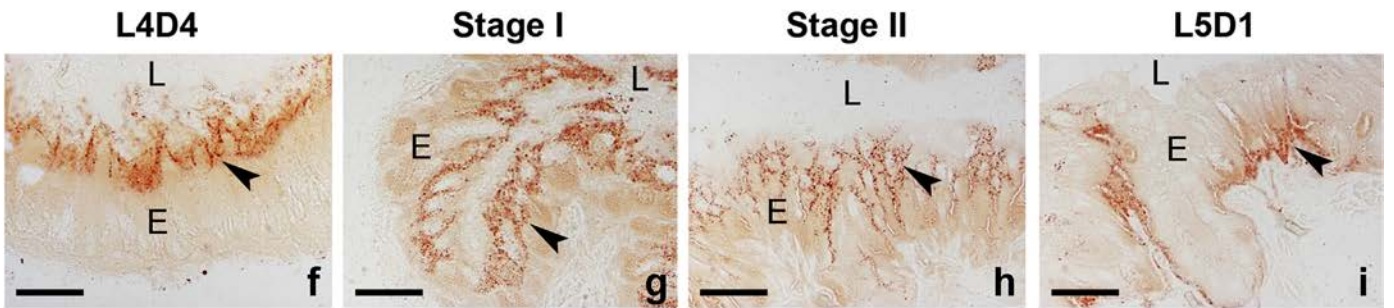
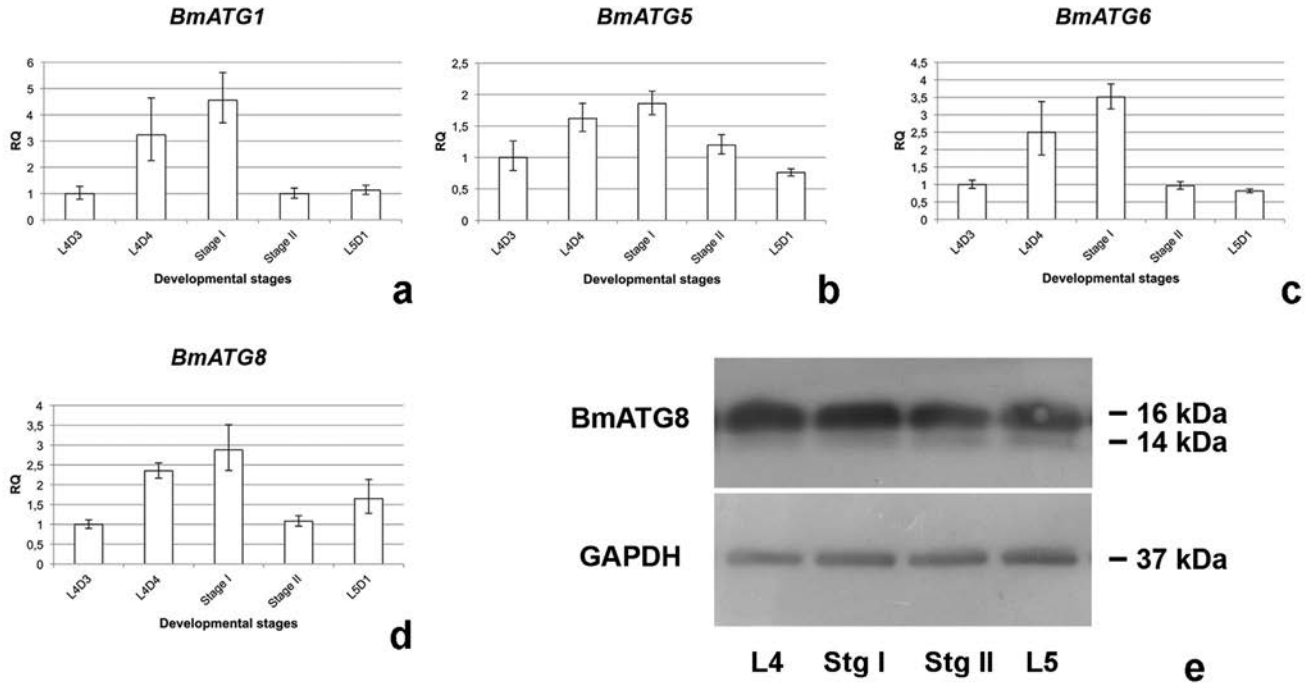


Fig. 5. Functional activity of the midgut. (a–d) Alkaline phosphatase. While a strong signal (arrowhead) is visible during fourth (a) and fifth (d) larval instar, the intensity of the staining is reduced during molt (b, c). (e) The activity of alkaline phosphatase was measured in midgut homogenates at different developmental stages (from L4D4 to L5D1). One-Way ANOVA ($F_{3,28} = 97.807$; $p < 0.0001$) and Tukey's post hoc test were used to compare the values. Statistically significant differences are denoted with different letters ($p < 0.0001$). Each bar represents mean \pm SE. (f) The activity of aminopeptidase N was measured in midgut homogenates at different developmental stages (from L4D4 to L5D1). One-Way ANOVA ($F_{3,28} = 52.727$; $p < 0.0001$) and Tukey's post hoc test were used to compare the values. Statistically significant differences are denoted with different letters (a,b $p < 0.003$; a,c and b,c $p < 0.0001$). Each bar represents mean \pm SE. (g–j) NADH-TR. The whole midgut epithelium is strongly stained for NADH-TR (blue) from L4D4 to L5D1. E: midgut epithelium; L: lumen. Bars 30 μ m (a–d, g–j). (For interpretation of the references to color in this figure legend, the reader is referred to the web version of this article.)

3.3. Analysis of autophagy and metabolic characterization of the midgut epithelium

Given that the functional activity of the midgut epithelium was partially reduced during molting, we characterized different aspects that are related to the metabolism of the epithelium during this 24 h-long starvation period. First we analyzed the occurrence of autophagy. In fact autophagy is rapidly triggered in eukaryotes when cells are deprived of nutrients. This process is suitable for digesting cytoplasm and organelles by recruiting lysosomal hydrolases and provides monomers to the cell that can be used for

anabolic or catabolic purposes. Since this autolytic process was also described in silkworm tissues during more or less prolonged starvation periods (Casati et al., 2012; Franzetti et al., 2012), and it was observed in the fat body during larva–larva molt (Tian et al., 2013), we decided to evaluate the activation of autophagy in midgut cells during molt. To this end we used multiple autophagic markers in accordance with the most recent guidelines on autophagy (Klionsky et al., 2016). Given that, according to previous observations obtained on silkworm midgut at the beginning of metamorphosis, the occurrence of autophagy is preceded by an increase in autophagy-related (ATG) gene transcription (Romanelli,



unpublished data), we performed the analysis of *BmATG1*, *BmATG5*, *BmATG6*, and *BmATG8* mRNA expression levels from the third day of the fourth larval instar. Real-time PCR quantification showed that mRNA levels of all these genes increased during the transition from the fourth larval instar to the molt (Fig. 6a–d). Despite the increased expression levels of these autophagic genes, western blot analysis of BmAtg8 did not detect any increase in autophagic activity. In fact, no variations in the intensity of the BmATG8–PE band, a protein that is specifically associated to autophagosome, were detected at any of the stages analyzed (Fig. 6e).

Given that our analysis did not reveal any autophagy activity in the midgut epithelium, we directed our attention to the tissue distribution of long-term energy storage nutrients, i.e., glycogen and lipids. While the amount of lipid droplets decreased slightly after molt was completed (as demonstrated by O.R.O. distribution) (Fig. 6f–i), the glycogen content of midgut cells decreased dramatically since the early stages of the molt (Fig. 6j–n). In particular, at L4D4 numerous glycogen deposits were distributed in the apical region of columnar cells (Fig. 6j), as also observed by TEM (Fig. 6o). Specificity of the PAS reaction towards glycogen was confirmed by treatment with diastase (Fig. 6k). These deposits decreased at early molt stage (stage I) (Fig. 6l) and disappeared almost completely at stage II (Fig. 6m). The glycogen content only began to increase again at the beginning of the fifth instar (Fig. 6n).

Collectively, this evidence suggests that, while autophagy is not activated, glycogen and, in part, lipid stores are mobilized in midgut cells during the larva–larva molt period.

4. Discussion

The present work aimed to investigate three specific aspects of larva–larva molt: i) the morphofunctional features of the midgut epithelial cells, with a particular focus on ISCs; ii) the metabolic and functional activity of the midgut tissue; and iii) the occurrence of autophagy in midgut cells.

4.1. Growth of midgut epithelium during molting

At the beginning of the molt period, when the larva has just stopped feeding, the midgut shows the typical features of a functional organ: it is formed by metabolically active columnar cells, which are full of mitochondria and characterized by a well-developed brush border, and goblet cells. Small groups of ISCs can be observed in the basal region of the epithelium. These cells are characterized by undifferentiated morphology and show a cytoplasm which is rich in ribosomes and mitochondria. As soon as the larva approaches stage I, the number of stem cells increases significantly, as shown by morphometric analysis. This ISC increase is confirmed by positivity of their nucleus for H3P, a marker that is able to identify cells undergoing mitosis. Western blot analysis showed that proliferation activity is essentially limited to the first half of the molt period (stage I). These data clearly demonstrate that stem cells proliferate massively once the larva enters the molting period. This evidence is in accordance with data obtained from Akai's group, which reported the occurrence of high levels of DNA synthesis at early molting stage in silkworm undergoing first and

second larva–larva molt (Akai, 1970; Akai and Park, 1971). In contrast, however, other studies performed on ISCs during larva–larva molting reported that, in Lepidoptera, this event occurs before molting, while stem cell differentiation intervenes later, once the molting process has already started (Smaghe et al., 2005; Corley and Lavine, 2006).

We have shown that, once ISCs have divided, some of them start to differentiate. These cells elongate towards the midgut lumen and, in those cells that become goblet cells, an inner cavity lined by microvilli appears. We were not able to discriminate the two rows of cells that differentiate into columnar and goblet cells, as described for *Manduca sexta* (Baldwin and Hakim, 1991b). This difference between the two insects further hinders the fine dissection of the differentiation process of new goblet and columnar cells from ISCs, a process that has been hypothesized so far only *in vitro* (Sadru-Din et al., 1996; Cerumenati et al., 2007).

While the cuticle is changed during the larva–larva molt (ecdysis), the membrane that surrounds the food bolus and protects the midgut epithelium (Moret and Moreau, 2012), i.e., the peritrophic matrix, is not lost. In fact, our morphological analysis demonstrates that this acellular sheath is maintained at all stages of the molting process. This is convenient for the larva since removal of the peritrophic matrix during molt would lead to a loss of residual food from the alimentary canal. Moreover, an intact peritrophic matrix not only preserves the larva from bacterial contamination, but can also support digestion processes during larva–larva molt. Indeed, several of our results suggest that functional activity in the midgut epithelium is maintained during molt: i) although alkaline phosphatase and N-aminopeptidase activity decreases during stage I and II, residual activity of the two enzymes is observed throughout the molt; ii) NADH-TR positivity persists at all stages, indicating that midgut cells remain metabolically active even during the molt period; and iii) the brush border of columnar cells does not seem to be affected by starvation, conversely to what was observed in *Drosophila* subjected to food deprivation (Li et al., 2009). All these data indicate that, although the larva does not feed for 24 h, the midgut functional activity is not interrupted during molt.

4.2. Metabolic characterization of the midgut epithelium during molting

Starvation is a potent stress that, in the insect midgut, determines a series of events such as mobilization of stored metabolites (Satake et al., 2000), misregulation of metabolic enzyme activity (Ban, 1974), shortening of microvilli (Li et al., 2009), and activation of compensatory mechanisms such as autophagy (Khoa and Takeda, 2012).

Since the functional activity of the midgut epithelium was partially reduced during the molting period, as discussed above, we investigated how metabolic activity within midgut cells is modified, in order to evaluate how they cope with starvation. To this aim we first analyzed the occurrence of autophagy in the epithelium. In fact, when the cell is subjected to nutrient deprivation, this cellular self-eating process can be activated to break down part of its reserves in order to stay alive until the

Fig. 6. Activation of autophagy and metabolic activity in the midgut epithelium during molt. (a–d) qRT-PCR analysis of autophagy-related genes. Expression of all four *ATG* genes has been increasing since L4D4. Data are represented as mean \pm SE. (e) Western blot analysis of BmATG8. The intensity of the band corresponding to BmATG8–PE (14-kDa) detected by the antibody does not show any increase throughout the molt. (f–i) O.R.O. Staining for O.R.O. (red, arrowhead) slightly decreases from stage II onwards. (j–n) PAS. Staining for PAS (magenta) reveals the presence of a significant amount of glycogen in the midgut epithelium during fourth larval instar (j, arrowheads). These glycogen deposits disappear after the treatment with diastase (k). As soon as the larva approaches stage I, glycogen granules progressively decrease (l, m). Glycogen content begins to increase again at L5D5 (n). (o) TEM micrograph showing large glycogen deposits (arrowheads) localized in the apical region of columnar cells (C). E: midgut epithelium; L: lumen; M: brush border; arrows: mitochondria. Bars 50 μ m (f–i), 30 μ m (j–n), 2 μ m (o). (For interpretation of the references to color in this figure legend, the reader is referred to the web version of this article.)

situation improves (He and Klionsky, 2009). In insects, as well as in other animal models, autophagy has been shown to be rapidly induced when the organism undergoes structural remodeling, such as during metamorphosis, or when cells need to generate intracellular nutrients and energy, e.g., during starvation (Tettamanti et al., 2007b; Malagoli et al., 2010; Romanelli et al., 2014). For example, in *Drosophila melanogaster*, a few hours of nutrient starvation induces autophagy in larval organs (Scott et al., 2004). Similarly in the silkworm, both larval midgut and fat body activate autophagy following forced nutrient starvation (Casati et al., 2012). Moreover, during larva–pupa transition in this insect, autophagy is activated as soon as the larva stops feeding to drive digestion of the larval midgut cells and degradation of complex molecules, thus providing nutrients to the newly forming pupal midgut (Franzetti et al., 2012). Finally, the expression of autophagic markers can be detected in the midgut and silk gland of *Galleria mellonella* when the larva is subjected to starvation, although their levels decrease after re-feeding (Khoa and Takeda, 2012). In our study, we did not observe a substantial activation of autophagy in midgut cells during larva–larva molting, as demonstrated by the BmAtg8–PE pattern throughout the molt. It is worthy of note that mRNA levels of the autophagic genes, observed in real-time PCR analysis, start to increase before the beginning of the molt. For this reason we assume that the transcriptional activation of these genes is triggered by ecdysteroids, whose levels in the hemolymph increase just before larva–larva molt (Zitnan and Adams, 2005), rather than by starvation. Our hypothesis is supported by the work performed by Tian and collaborators (Tian et al., 2013), who described a 20E response element in the BmATG1 promoter region and showed that other BmATG genes proved to be potentially 20E-primary-responsive. In any case, a full autophagic response cannot be switched on simply by activating autophagic gene transcription in the midgut. This limitation cannot be overcome by the starvation stimulus, probably due to the short duration of nutrient starvation (only 24 h) and to the presence of residual food in the alimentary canal that can supply nutrients, at least in the first part of the molt period. This result is in accordance with what we previously observed in the silkworm subjected to forced starvation (Casati et al., 2012). In fact, in that situation, the midgut epithelium required at least 96 h to trigger autophagy after being deprived of nutrients; conversely, the activation of autophagy was stronger and faster in the fat body (24 h from the beginning of the starvation protocol), thus confirming this organ to be a highly responsive tissue following nutrient deprivation (Colombani et al., 2003).

Given that our data did not demonstrate activation of the autophagic process, we analyzed the distribution of lipids and carbohydrates, the two main long-storage molecules that are present in eukaryotic cells. Histochemical and ultrastructural analyses showed that, while abundant glycogen reserves and lipid droplets are visible in midgut cells at L4D4, these are degraded as soon as molting proceeds. A similar behavior was previously observed in the midgut epithelium of silkworms deprived of food (Satake et al., 2000). These data collectively demonstrate that midgut cells draw heavily on stored reserve molecules instead of activating autophagy to survive starvation.

In summary, our work demonstrated that: i) ISCs mainly proliferate during the first half of the molt period to widen the midgut epithelium; ii) the overall structure of the midgut epithelium is maintained and its functional activity is partially retained throughout the molt; and iii) midgut cells do not need autophagy to cope with nutrient deprivation, as long-term energy storage nutrients are mobilized and provide a trophic support to the midgut epithelium during the starvation period.

Acknowledgments

The authors wish to thank Dr. Muthukumaran Rajagopalan who participated in early experiments and Daniele Bruno for technical assistance. We thank Sherryl Sundell for English editing. This work was partially supported by FAR 2014 (University of Insubria) to GT.

References

- Akai, H., 1970. An electron microscopy study of the alimentary canal of the silkworm *Bombyx mori* L. I. The ultrastructure of the midgut epithelium. *Bull. Seric. Exp. Stn.* 24, 303–344.
- Akai, H., Park, K.J., 1971. Nucleic acid synthesis in various tissues during the larval molting cycle of *Bombyx mori* L. (Lepidoptera: Bombycidae). *Appl. Entomol. Zool.* 6, 63–66.
- Baldwin, K., Hakim, R.S., 1991a. Cell proliferation and maintenance of pattern during molting in midgut of tobacco hornworm. *Anat. Rec.* 229, 7A–8A.
- Baldwin, K.M., Hakim, R., Loeb, M., Sadrud-Din, S., 1996. Midgut development. In: Lehane, M.J., Billingsley, P.F. (Eds.), *Biology of the Insect Midgut*. Chapman & Hall, London, pp. 31–54.
- Baldwin, K.M., Hakim, R.S., 1991b. Growth and differentiation of the larval midgut epithelium during molting in the moth, *Manduca sexta*. *Tissue Cell* 23, 411–422.
- Baldwin, K.M., Hakim, R.S., Stanton, G.B., 1993. Cell-cell communication correlates with pattern formation in molting *Manduca* midgut epithelium. *Dev. Dyn.* 197, 239–243.
- Ban, D., 1974. Influence of starvation on metabolic activities of the midgut epithelium of *Galleria mellonella* larvae. *Folia Histochem. Cytochem.* 12, 145–156.
- Blackburn, M.B., Loeb, M.J., Clark, E., Jaffe, H., 2004. Stimulation of midgut stem cell proliferation by *Manduca sexta* alpha-arylophorin. *Arch. Insect Biochem. Physiol.* 55, 26–32.
- Cappelozza, L., Cappelozza, S., Saviane, A., Sbrenna, G., 2005. Artificial diet rearing system for the silkworm *Bombyx mori* (Lepidoptera: Bombycidae): effect of vitamin C deprivation on larval growth and cocoon production. *Appl. Entomol. Zool.* 40, 405–412.
- Casartelli, M., Cermenati, G., Rodighiero, S., Pennacchio, F., Giordana, B., 2008. A megalin-like receptor is involved in protein endocytosis in the midgut of an insect (*Bombyx mori*, Lepidoptera). *Am. J. Physiol. Regul. Integr. Comp. Physiol.* 295, R1290–R1300.
- Casartelli, M., Corti, P., Cermenati, G., Grimaldi, A., Fiandra, L., Santo, N., Pennacchio, F., Giordana, B., 2007. Absorption of horseradish peroxidase in *Bombyx mori* larval midgut. *J. Insect Physiol.* 53, 517–525.
- Casati, B., Terova, G., Cattaneo, A.G., Rimoldi, S., Franzetti, E., de Eguileor, M., Tettamanti, G., 2012. Molecular cloning, characterization and expression analysis of ATG1 in the silkworm, *Bombyx mori*. *Gene* 511, 326–337.
- Cermenati, G., Corti, P., Caccia, S., Giordana, B., Casartelli, M., 2007. A morphological and functional characterization of *Bombyx mori* larval midgut cells in culture. *Invert. Surviv. J.* 4, 119–126.
- Colombani, J., Raisin, S., Pantalacci, S., Radimerski, T., Montagne, J., Leopold, P., 2003. A nutrient sensor mechanism controls *Drosophila* growth. *Cell* 114, 739–749.
- Corley, L.S., Lavine, M.D., 2006. A review of insect stem cell types. *Semin. Cell Dev. Biol.* 17, 510–517.
- Dow, J.A.T., 1986. Insect midgut function. *Adv. Insect Physiol.* 19, 187–328.
- Franzetti, E., Huang, Z.J., Shi, Y.X., Xie, K., Deng, X.J., Li, J.P., Li, Q.R., Yang, W.Y., Zeng, W.N., Casartelli, M., Deng, H.M., Cappelozza, S., Grimaldi, A., Xia, Q., Feng, Q., Cao, Y., Tettamanti, G., 2012. Autophagy precedes apoptosis during the remodeling of silkworm larval midgut. *Apoptosis* 17, 305–324.
- Franzetti, E., Romanelli, D., Caccia, S., Cappelozza, S., Congiu, T., Rajagopalan, M., Grimaldi, A., de Eguileor, M., Casartelli, M., Tettamanti, G., 2015. The midgut of the silkworm *Bombyx mori* is able to recycle molecules derived from degeneration of the larval midgut epithelium. *Cell Tissue Res.* 361, 509–528.
- Gullan, P.J., Cranston, P.S., 2014. *The Insects: an Outline of Entomology*. Wiley-Blackwell, Chichester, pp. 156–189.
- Hakim, R.S., Baldwin, K., Smagghe, G., 2010. Regulation of midgut growth, development, and metamorphosis. *Annu. Rev. Entomol.* 55, 593–608.
- Hakim, R.S., Caccia, S., Loeb, M., Smagghe, G., 2009. Primary culture of insect midgut cells. *Vitro Cell Dev. Biol. Anim.* 45, 106–110.
- He, C.C., Klionsky, D.J., 2009. Regulation mechanisms and signaling pathways of autophagy. *Annu. Rev. Genet.* 43, 67–93.
- Khoa, D.B., Takeda, M., 2012. Expression of autophagy 8 (Atg8) and its role in the midgut and other organs of the greater wax moth, *Galleria mellonella*, during metamorphic remodelling and under starvation. *Insect Mol. Biol.* 21, 473–487.
- Klionsky, D.J., Abdelmohsen, K., Abe, et al., 2016. Guidelines for the use and interpretation of assays for monitoring autophagy. *Autophagy* 12, 1–222.
- Li, H.M., Sun, L., Mittapalli, O., Muir, W.M., Xie, J., Wu, J., Schemerhorn, B.J., Sun, W., Pittendrigh, B.R., Murdock, L.L., 2009. Transcriptional signatures in response to wheat germ agglutinin and starvation in *Drosophila melanogaster* larval midgut. *Insect Mol. Biol.* 18, 21–31.
- Loeb, M.J., Coronel, N., Natsukawa, D., Takeda, M., 2004. Implications for the functions of the four known midgut differentiation factors: an immunohistologic study of *Heliothis virescens* midgut. *Arch. Insect Biochem. Physiol.* 56, 7–20.
- Malagoli, D., Abdalla, F.C., Cao, Y., Feng, Q.L., Fujisaki, K., Gregorc, A., Matsuo, T., Nezis, I.P., Papassideri, I.S., Sass, M., Silva-Zacarin, E.C.M., Tettamanti, G.,

- Umemiya-Shirafuji, R., 2010. Autophagy and its physiological relevance in arthropods: current knowledge and perspectives. *Autophagy* 6, 575–588.
- Miao, D., Scutt, A., 2002. Histochemical localization of alkaline phosphatase activity in decalcified bone and cartilage. *J. Histochem. Cytochem.* 50, 333–340.
- Moret, Y., Moreau, J., 2012. The immune role of the arthropod exoskeleton. *Invert. Surviv. J.* 9, 200–206.
- Riddiford, L.M., Hiruma, K., Zhou, X., Nelson, C.A., 2003. Insights into the molecular basis of the hormonal control of molting and metamorphosis from *Manduca sexta* and *Drosophila melanogaster*. *Insect Biochem. Mol. Biol.* 33, 1327–1338.
- Romanelli, D., Casati, B., Franzetti, E., Tettamanti, G., 2014. A molecular view of autophagy in Lepidoptera. *BioMed Res. Int.* 2014, 902315.
- Rost-Roszkowska, M., Chechelska, A., Fradczak, M., Salitra, K., 2008. Ultrastructure of two types of endocrine cells in the midgut epithelium of *Spodoptera exiqua* Hubner, 1808 (Insecta, Lepidoptera, Noctuidae). *Zool. Pol.* 53, 27–35.
- Sadrud-Din, S., Loeb, M., Hakim, R., 1996. In vitro differentiation of isolated stem cells from the midgut of *Manduca sexta* larvae. *J. Exp. Biol.* 199, 319–325.
- Satake, S., Kawabe, Y., Mizoguchi, A., 2000. Carbohydrate metabolism during starvation in the silkworm *Bombyx mori*. *Arch. Insect Biochem. Physiol.* 44, 90–98.
- Scott, R.C., Schuldiner, O., Neufeld, T.P., 2004. Role and regulation of starvation-induced autophagy in the *Drosophila* fat body. *Dev. Cell* 7, 167–178.
- Sehnal, F., Zitnan, D., 1996. Midgut Endocrine Cells. In: Lehane, M.J., Billingsley, P.F. (Eds.), *Biology of the insect midgut*, London, pp. 55–85.
- Smagghe, G.J., Elsen, K., Loeb, M.J., Gelman, D.B., Blackburn, M., 2003. Effects of a fat body extract on larval midgut cells and growth of lepidoptera. *Vitro Cell Dev. Biol. Anim.* 39, 8–12.
- Smagghe, G., Vanhassel, W., Moeremans, C., De Wilde, D., Goto, S., Loeb, M., Blackburn, M., Hakim, R., 2005. Stimulation of midgut stem cell proliferation and differentiation by insect hormones and peptides. *Ann. N. Y. Acad. Sci.* 1040, 472–475.
- Terra, W.R., Ferreira, C., 1994. Insect digestive enzymes: properties, compartmentalization and function. *Comp. Biochem. Physiol. B* 109, 1–62.
- Terra, W.R., Ferreira, C., 2005. Biochemistry of digestion. In: Gilbert, L.I., Iatrou, K., Gill, S.S. (Eds.), *Comprehensive Molecular Insect Science*. Elsevier Pergamon Press, Oxford, pp. 171–224.
- Tettamanti, G., Grimaldi, A., Casartelli, M., Ambrosetti, E., Ponti, B., Congiu, T., Ferrarese, R., Rivas-Pena, M.L., Pennacchio, F., Eguileor, M., 2007a. Programmed cell death and stem cell differentiation are responsible for midgut replacement in *Heliothis virescens* during prepupal instar. *Cell Tissue Res.* 330, 345–359.
- Tettamanti, G., Grimaldi, A., Pennacchio, F., de Eguileor, M., 2007b. Lepidopteran larval midgut during prepupal instar: digestion or self-digestion? *Autophagy* 3, 630–631.
- Tettamanti, G., Grimaldi, A., Pennacchio, F., de Eguileor, M., 2008. *Toxoneuron nigriceps* parasitization delays midgut replacement in fifth-instar *Heliothis virescens* larvae. *Cell Tissue Res.* 332, 371–379.
- Tian, L., Ma, L., Guo, E., Deng, X., Ma, S., Xia, Q., Cao, Y., Li, S., 2013. 20-hydroxyecdysone upregulates Atg genes to induce autophagy in the *Bombyx* fat body. *Autophagy* 9, 1172–1187.
- Uwo, M.F., Ui-Tei, K., Park, P., Takeda, M., 2002. Replacement of midgut epithelium in the greater wax moth, *Galleria mellonella*, during larval-pupal moult. *Cell Tissue Res.* 308, 319–331.
- Wigglesworth, V.B., 1972. *The Principles of Insect Physiology*. Chapman & Hall, London, pp. 61–145.
- Zhao, X.F., He, H.J., Dong, D.J., Wang, J.X., 2006. Identification of differentially expressed proteins during larval molting of *Helicoverpa armigera*. *J. Proteome Res.* 5, 164–169.
- Zitnan, D., Adams, M.E., 2005. Neuroendocrine regulation of insect ecdysis. In: Gilbert, L.I., Iatrou, K., Gill, S.S. (Eds.), *Comprehensive Molecular Insect Science*. Elsevier – Pergamon, Oxford, pp. 1–60.